Stem Cell Reports, Volume *9*

Supplemental Information

Functional Antagonism between OTX2 and NANOG Specifies a Spectrum of Heterogeneous Identities in Embryonic Stem Cells

Dario Acampora, Luca Giovanni Di Giovannantonio, Arcomaria Garofalo, Vincenzo Nigro, Daniela Omodei, Alessia Lombardi, Jingchao Zhang, Ian Chambers, and Antonio Simeone

SUPPLEMENTAL INFORMATION

Functional antagonism between OTX2 and NANOG specifies a spectrum of heterogeneous identities in embryonic stem cells

Dario Acampora, Luca Giovanni Di Giovannantonio, Arcomaria Garofalo, Vincenzo Nigro, Daniela Omodei, Alessia Lombardi, Jingchao Zhang, Ian Chambers and Antonio Simeone

SUPPLEMENTAL FIGURES

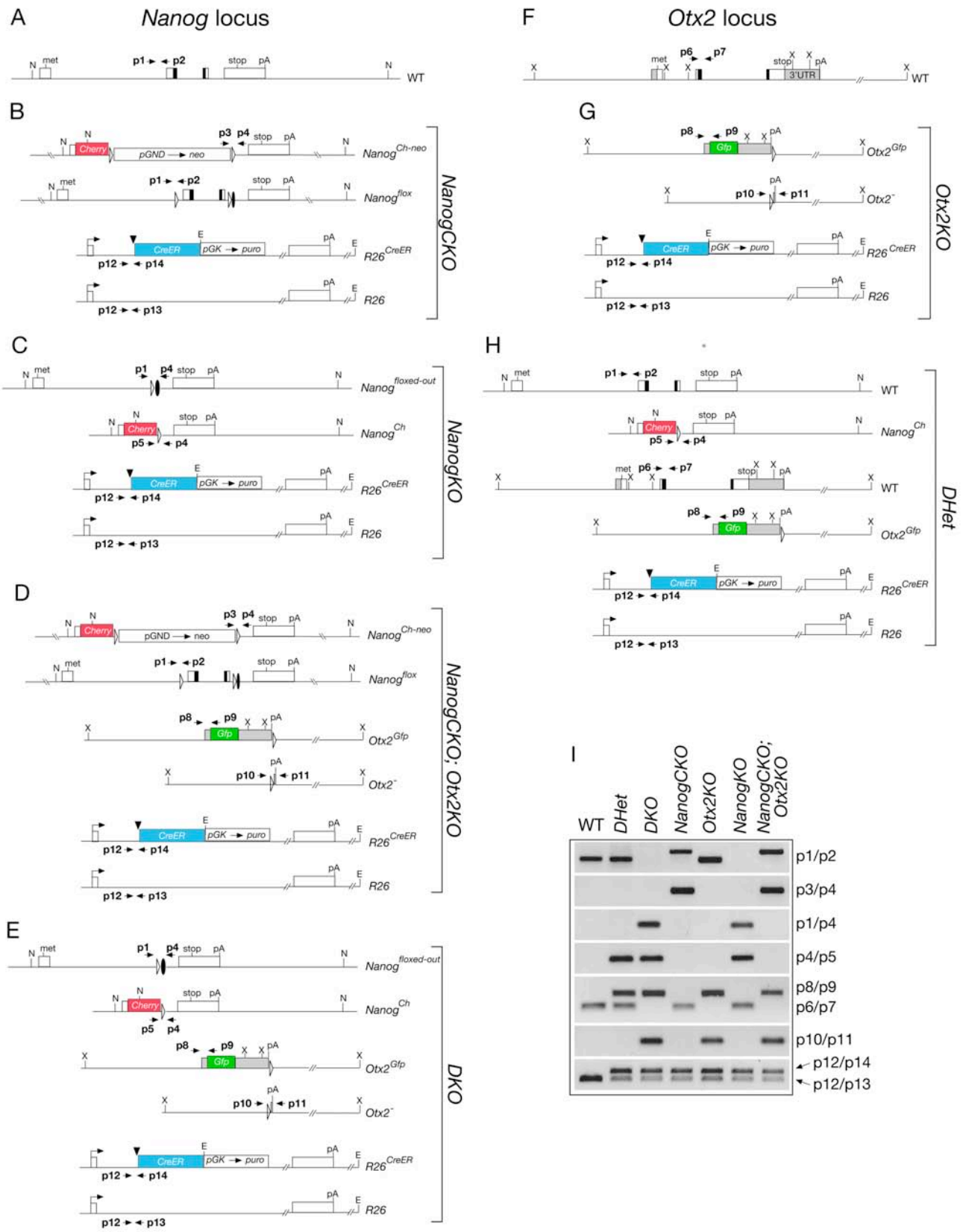

Figure S1. Generation of mutant ESC lines, related to Figures 1, S2 and 2. (A-H) Schematic representation of the *Nanog* and *Otx2* WT (A,F) and targeted loci (B-E, G,H); for each mutant ESC line only the final alleles are shown. (I) Allele-specific PCRs of the final ESC lines with the primers indicated as p1-14 in (A-H). Open arrowheads indicate *loxP* sites. Filled ovals indicate FRT sites. N, E and X stand for *NcoI,* EcoRI and *XbaI* restriction enyzymes; pA indicates the poly A addition site; the red, green and pale blue boxes correspond to *Ch*, *Gfp* and *CreER* genes, respectively.

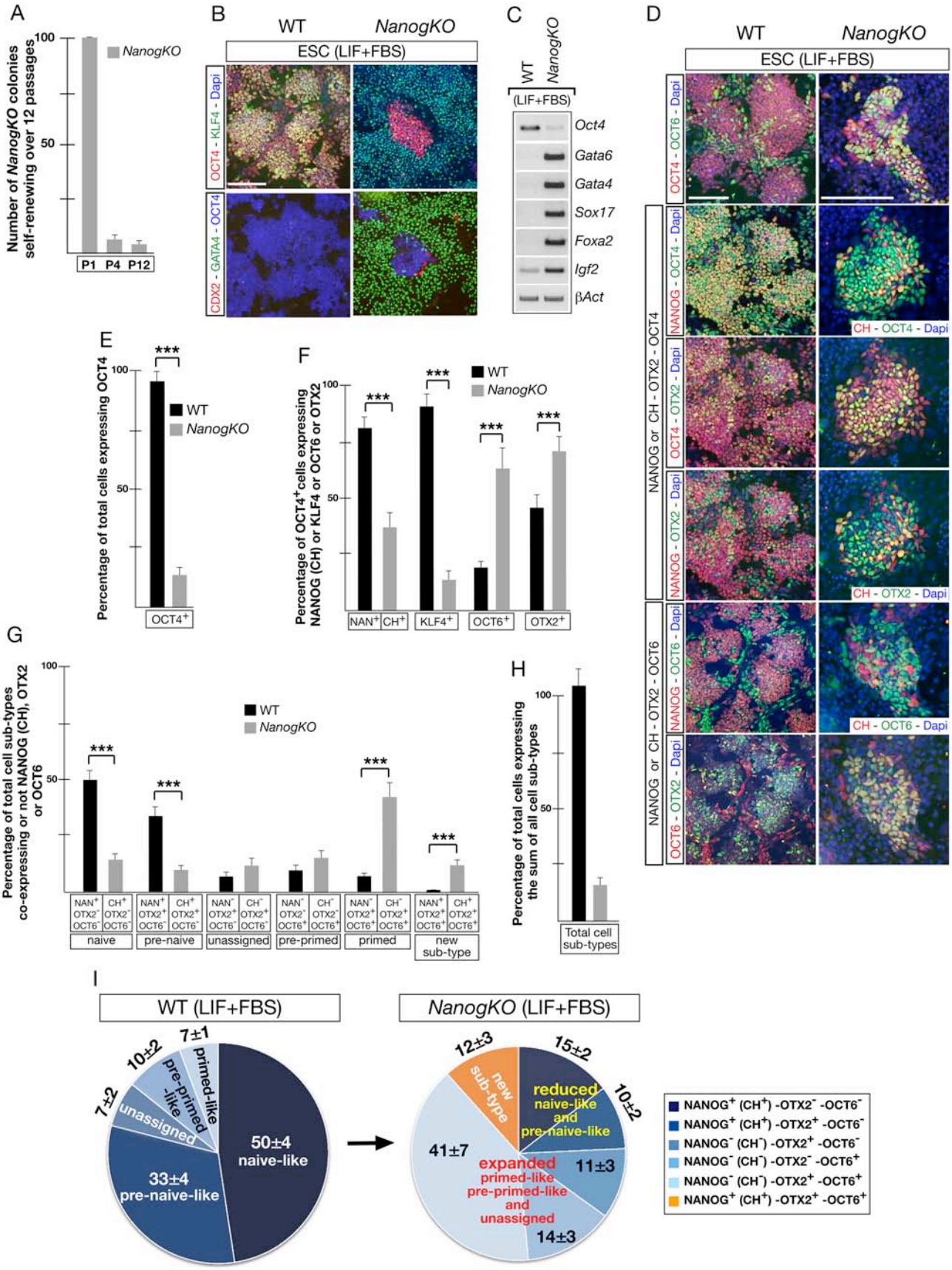

Figure S2. ***NanogKO*** **ESCs show impaired self-renewal and expanded expression of OTX2 and OCT6, related to Figure 1.** (A) Graphic representation showing the number of *NanogKO* ESCs colonies self-renewing at P12. Data are presented as mean ± SD from 3 independent experiments. (B) Representative images of WT and *NanogKO* ESCs immunostained with OCT4 and KLF4 and with CDX2, GATA4 and OCT4. (C) RT-PCR assays with *Oct4*, *Gata6*, *Gata4*, *Sox17*, *Foxa2*, *Igf2* on RNAs normalized by *β-Actin* expression showing heavy reduction of *Oct4* and abundant PE-like differentiation (n=3 independent experiments). (D) Representative images of WT and *NanogKO* ESCs immunostained with OCT4 and OCT6, with NANOG or CH, OTX2 and OCT4 and with NANOG or CH, OTX2 and OCT6 showing the remarkable increase in the number of $OCT4^+$ cells co-expressing OTX2 and OCT6 and the decrease of those CH^+. Cells are

also stained with Dapi. Scale bars correspond to 100µM. (E-H) Graphic representation of cell counting analysis showing in WT and *NanogKO* ESCs the percentage of total cells expressing OCT4 (E), the percentage of $OCT4^{+}$ cells co-expressing NANOG or CH, KLF4, OCT6 and OTX2 (F), the percentage of total cell sub-types expressing naïve-like, pre-naive-like, unassigned, pre-primed-like, primed-like and a new sub-type absent in WT ESCs (G), and the percentage of total cells expressing the sum of cells belonging to all sub-types (H). Data are presented as mean ± SD from 4 independent experiments; *P* value: ***= <<0,001. (I) Schematic representation showing that compared to WT, *NanogKO* ESCs show a remarkable re-distribution of sub-type compartments with a severe reduction of naïve-like and pre-naïve-like compartments and a marked expansion of the primed-like compartment. A color code of the different sub-type compartments is shown.

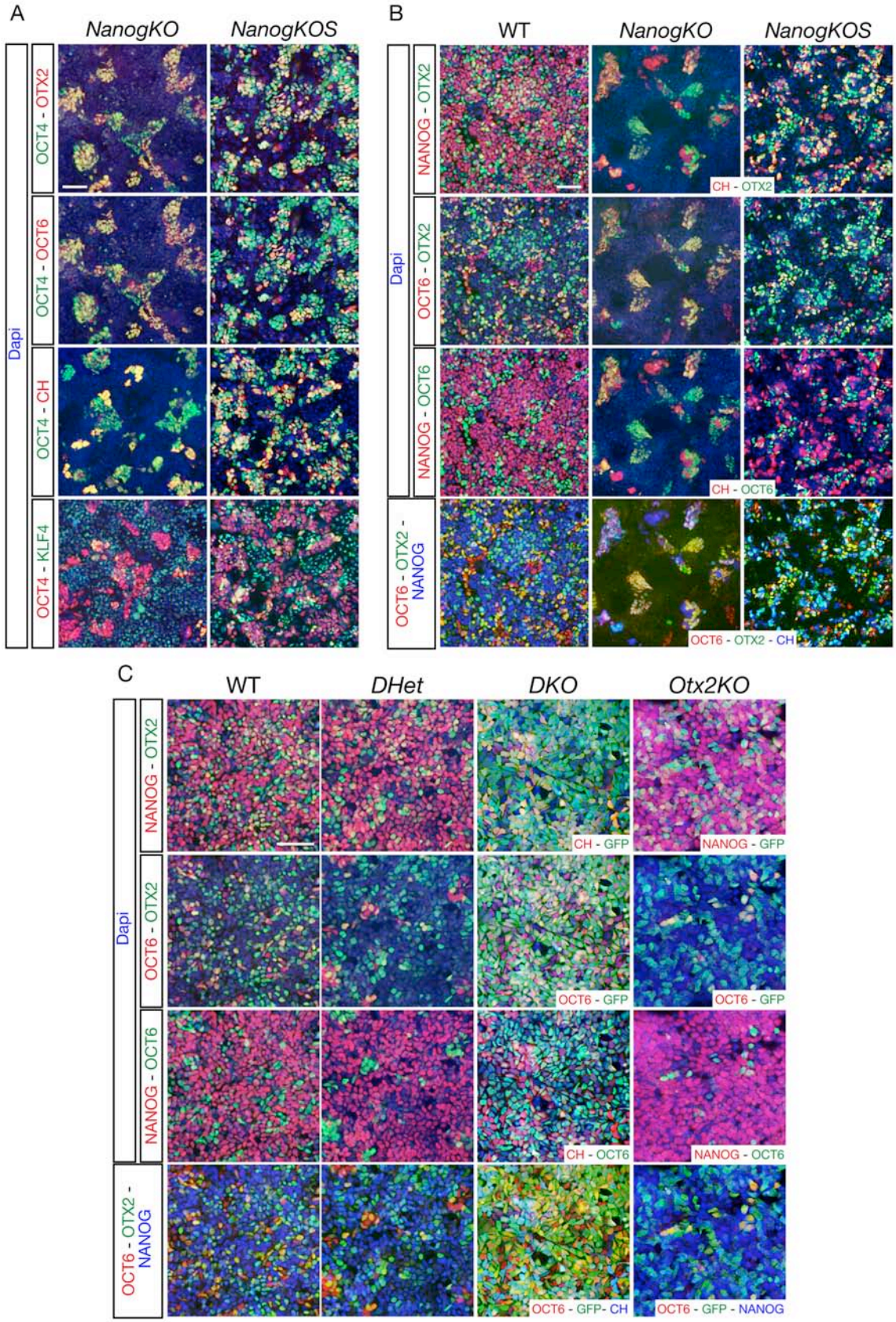

Figure S3. Immunohistochemistry experiments for cell counting analysis in mutant ESCs, related to Figures 1, 3 and S2. (A) Representative immunostaining assays performed on *NanogKO* and *NanogKOS* ESCs to determine the number of $OCT4^+$ cells and that of $OCT4^+$ cells co-expressing OTX2 or OCT6 or KLF4 or CH. (B) Representative immunostainings performed on WT, *NanogKO* and *NanogKOS* cells with NANOG or CH, OTX2 and OCT6 to determine the numerical size of sub-type compartments. (C) Representative immunostaining assays performed on WT, *DHet*, *DKO* and *Otx2KO* ESCs with NANOG or CH, OTX2 or GFP and OCT6 to determine the number of naïve-like, pre-naïve-like, unassigned, pre-primed-like and primed-like sub-type compartments. Scale bar in (A, B) corresponds to 100µM, and in (C) to 50µM. See also Tables S1 and S2.

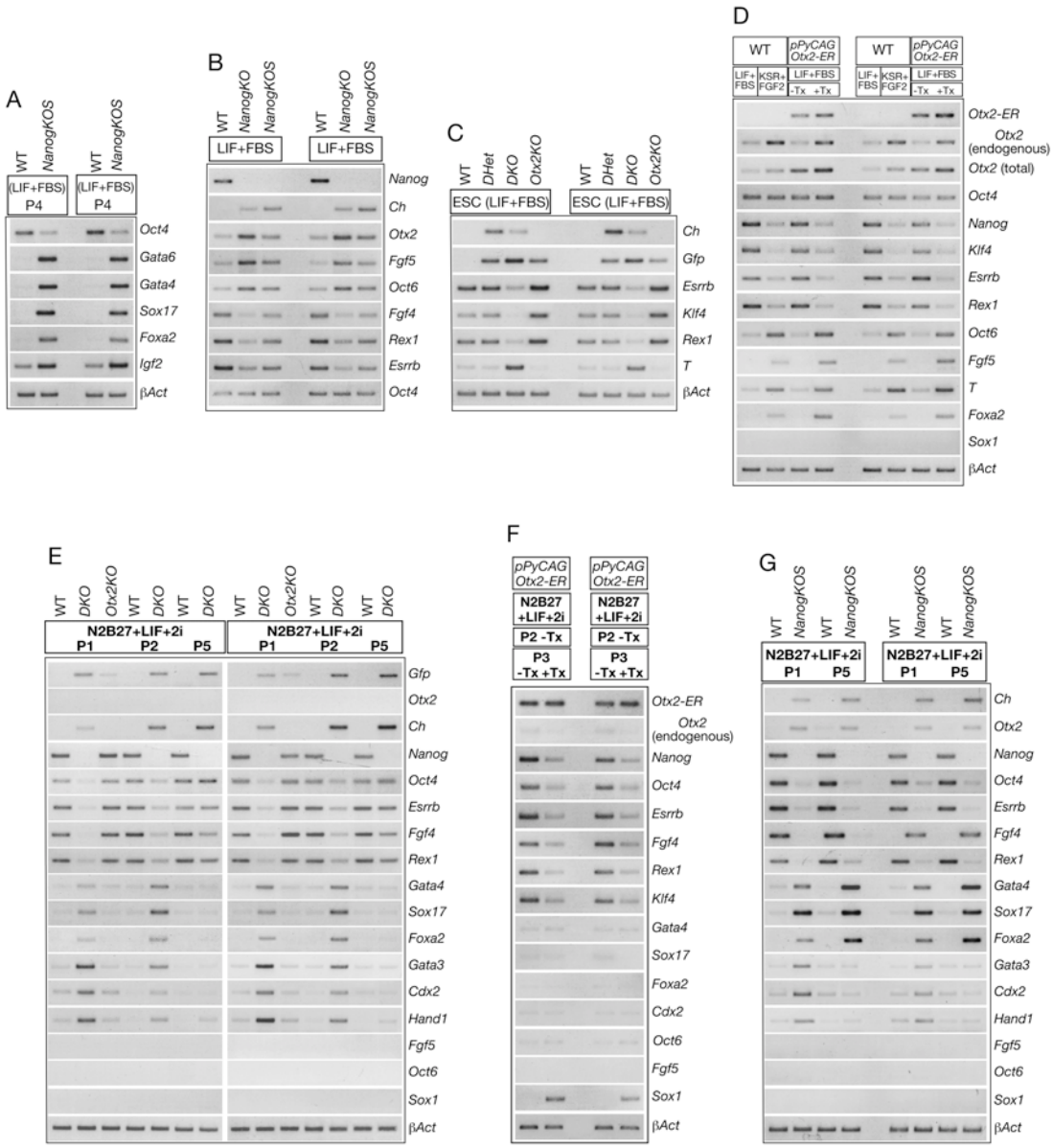

Figure S4. RT-PCR replicated assays, related to Figures 1, 2, 6 and 7. (A-G) RT-PCR experiments from two additional and independent experiments performed for gene transcripts shown in Figures 1D (A), 1J (B), 2F (C), 6B (D), 7B (E), 7E (F), and 7G (G).

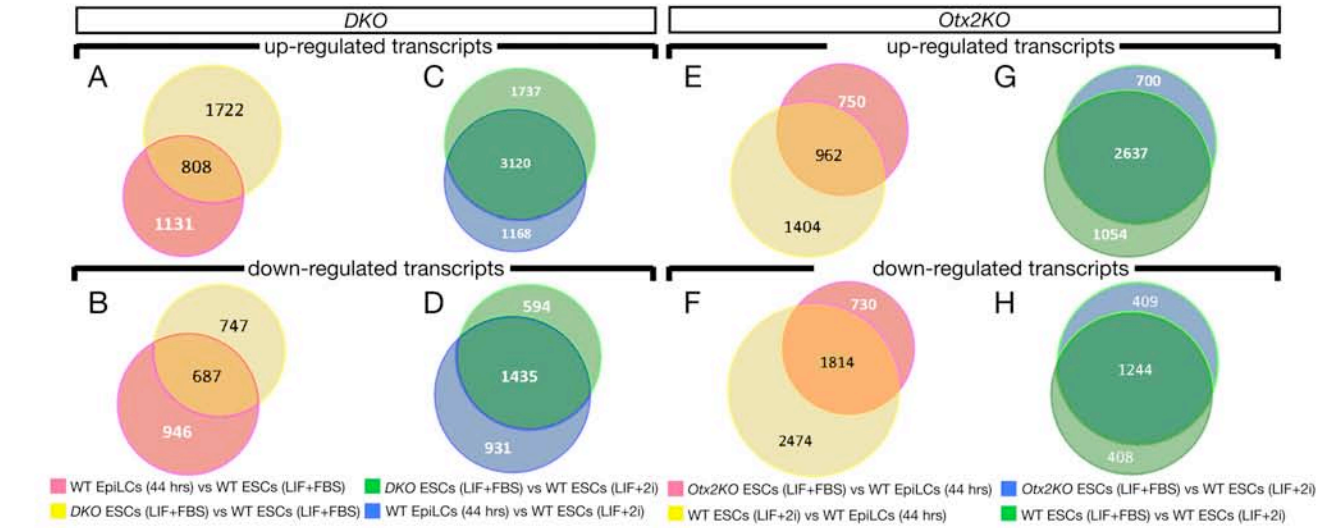
DKO
Otx2KO
up-regulated transcripts
down-regulated transcripts
A
1722
808
1131
C
1737
3120
1168
E
750
962
1404
G
700
2637
1054
B
747
687
946
D
594
1435
931
F
730
1814
2474
H
409
1244
408
WT EpiLCs (44 hrs) vs WT ESCs (LIF+FBS)
DKO ESCs (LIF+FBS) vs WT ESCs (LIF+2i)
Otx2KO ESCs (LIF+FBS) vs WT EpiLCs (44 hrs)
Otx2KO ESCs (LIF+FBS) vs WT ESCs (LIF+2i)
DKO ESCs (LIF+FBS) vs WT ESCs (LIF+FBS)
WT EpiLCs (44 hrs) vs WT ESCs (LIF+2i)
WT ESCs (LIF+2i) vs WT EpiLCs (44 hrs)
WT ESCs (LIF+FBS) vs WT ESCs (LIF+2i)

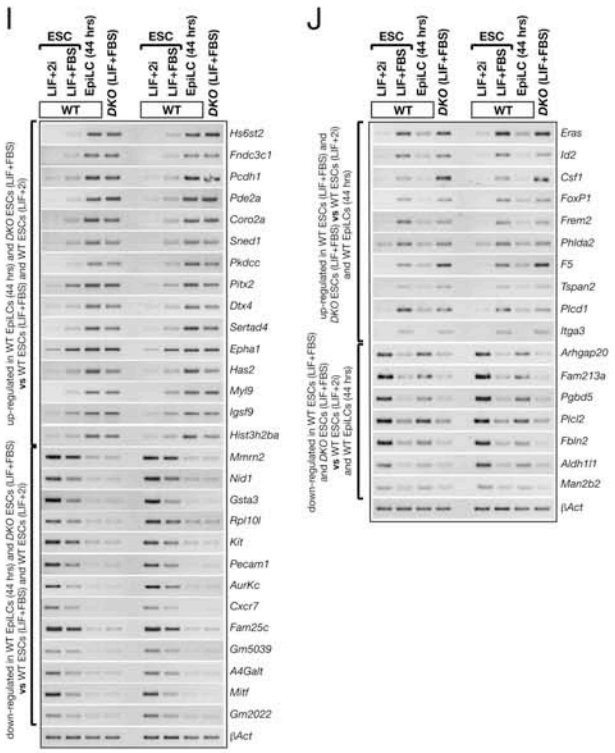
I
ESC
LIF+2i
LIF+FBS
EpiLC (44 hrs)
DKO (LIF+FBS)
WT
Hs6st2
Fndc3c1
Pcdh1
Pde2a
Coro2a
Sned1
Pkdcc
Pitx2
Dtx4
Sertad4
Epha1
Has2
Myl9
Igsf9
Hist3h2ba
Mmrn2
Nid1
Gsta3
Rpl10l
Kit
Pecam1
AurKc
Cxcr7
Fam25c
Gm5039
A4Galt
Mitf
Gm2022
βAct
up-regulated in WT EpiLCs (44 hrs) and DKO ESCs (LIF+FBS) vs WT ESCs (LIF+FBS) and WT ESCs (LIF+2i)
down-regulated in WT EpiLCs (44 hrs) and DKO ESCs (LIF+FBS) vs WT ESCs (LIF+FBS) and WT ESCs (LIF+2i)

J
Eras
Id2
Csf1
FoxP1
Frem2
Phlda2
F5
Tspan2
Plcd1
Itga3
Arhgap20
Fam213a
Pgbd5
Plcl2
Fbln2
Aldh1l1
Man2b2
βAct
up-regulated in WT ESCs (LIF+FBS) and DKO ESCs (LIF+FBS) vs WT ESCs (LIF+2i) and WT EpiLCs (44 hrs)
down-regulated in WT ESCs (LIF+FBS) and DKO ESCs (LIF+FBS) vs WT ESCs (LIF+2i) and WT EpiLCs (44 hrs)

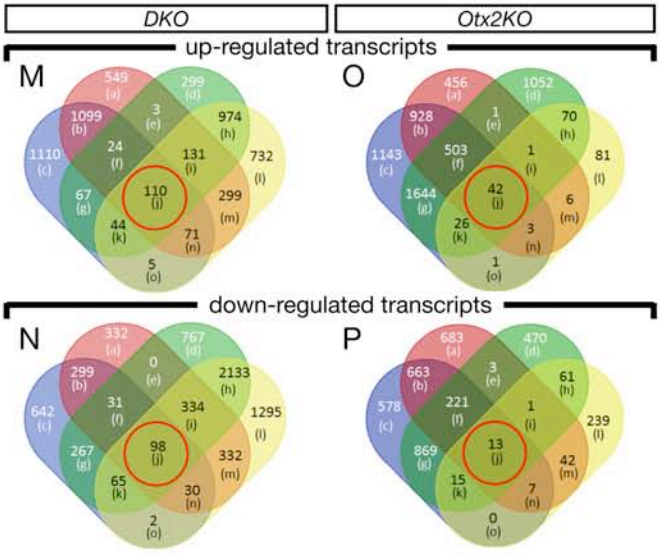
DKO
Otx2KO
up-regulated transcripts
down-regulated transcripts
M
549 (a)
299 (d)
1099 (b)
3 (e)
974 (h)
1110 (c)
24 (f)
131 (i)
732 (l)
67 (g)
110 (j)
299 (m)
44 (k)
71 (n)
5 (o)
O
456 (a)
1052 (d)
928 (b)
1 (e)
70 (h)
1143 (c)
503 (f)
1 (i)
81 (l)
1644 (g)
42 (j)
6 (m)
26 (k)
3 (n)
1 (o)
N
332 (a)
767 (d)
299 (b)
0 (e)
2133 (h)
642 (c)
31 (f)
334 (i)
1295 (l)
267 (g)
98 (j)
332 (m)
65 (k)
30 (n)
2 (o)
P
683 (a)
470 (d)
663 (b)
3 (e)
61 (h)
578 (c)
221 (f)
1 (i)
239 (l)
869 (g)
13 (j)
42 (m)
15 (k)
7 (n)
0 (o)
DKO ESCs (LIF+FBS) vs WT ESCs (LIF+FBS)
DKO ESCs (LIF+FBS) vs WT EpiLCs (44 hrs)
WT ESCs (LIF+2i) vs WT EpiLCs (44 hrs)
WT ESCs (LIF+2i) vs WT ESCs (LIF+FBS)
WT EpiLCs (44 hrs) vs WT ESCs (LIF+2i)
WT EpiLCs (44 hrs) vs WT ESCs (LIF+FBS)
Otx2KO ESCs (LIF+FBS) vs WT ESCs (LIF+FBS)
Otx2KO ESCs (LIF+FBS) vs WT ESCs (LIF+2i)

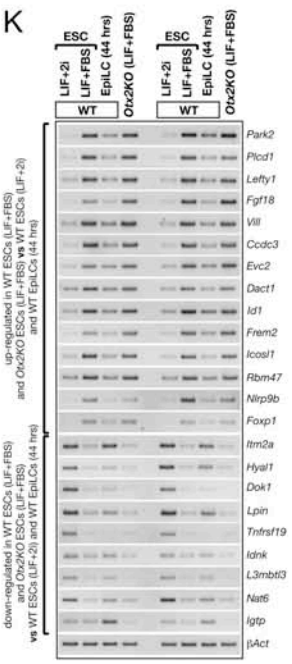
K
ESC
LIF+2i
LIF+FBS
EpiLC (44 hrs)
Otx2KO (LIF+FBS)
WT
Park2
Plcd1
Lefty1
Fgf18
Vill
Ccdc3
Evc2
Dact1
Id1
Frem2
Icosl1
Rbm47
Nlrp9b
Foxp1
Itm2a
Hyal1
Dok1
Lpin
Tnfrsf19
Idnk
L3mbtl3
Nat6
Igtp
βAct
up-regulated in WT ESCs (LIF+FBS) and Otx2KO ESCs (LIF+FBS) vs WT ESCs (LIF+2i) and WT EpiLCs (44 hrs)
down-regulated in WT ESCs (LIF+FBS) and Otx2KO ESCs (LIF+FBS) vs WT ESCs (LIF+2i) and WT EpiLCs (44 hrs)

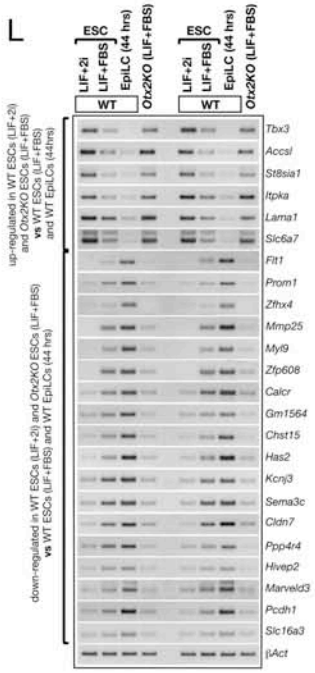
L
ESC
LIF+2i
LIF+FBS
EpiLC (44 hrs)
Otx2KO (LIF+FBS)
WT
Tbx3
Accsl
St8sia1
Itpka
Lama1
Slc6a7
Flt1
Prom1
Zfhx4
Mmp25
Myl9
Zfp608
Calcr
Gm1564
Chst15
Has2
Kcnj3
Sema3c
Cldn7
Ppp4r4
Hivep2
Marveld3
Pcdh1
Slc16a3
βAct
up-regulated in WT ESCs (LIF+2i) and Otx2KO ESCs (LIF+FBS) vs WT ESCs (LIF+FBS) and WT EpiLCs (44hrs)
down-regulated in WT ESCs (LIF-2i) and Otx2KO ESCs (LIF+FBS) vs WT ESCs (LIF+FBS) and WT EpiLCs (44 hrs)

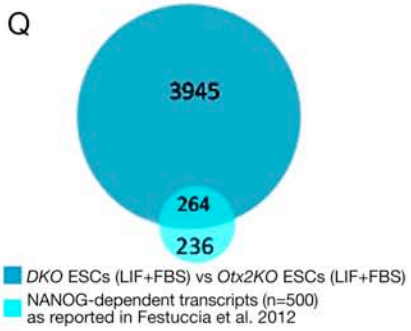
Q
3945
264
236
DKO ESCs (LIF+FBS) vs Otx2KO ESCs (LIF+FBS)
NANOG-dependent transcripts (n=500)
as reported in Festuccia et al. 2012

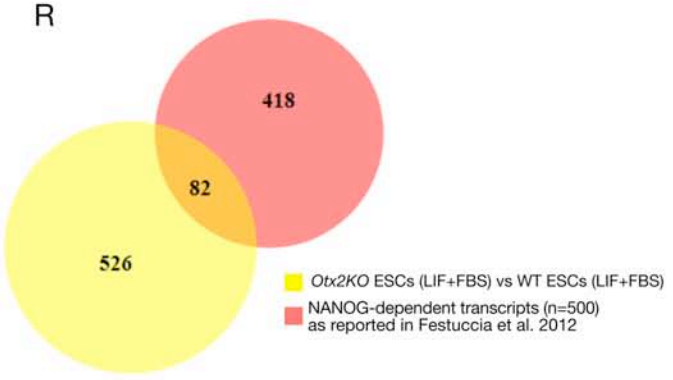
R
418
82
526
Otx2KO ESCs (LIF+FBS) vs WT ESCs (LIF+FBS)
NANOG-dependent transcripts (n=500)
as reported in Festuccia et al. 2012

Figure S5. Transcriptomic analysis of *DKO* and *Otx2KO* ESCs, related to Figure 4. (A-H) Pairwise Venn diagrams showing differentially expressed genes between *DKO* ESCs (LIF+FBS) and WT EpiLCs (44 hrs) both compared to WT ESCs (LIF+FBS) (A, B) and to WT ESCs (LIF+2i) (C, D); and pairwise Venn diagrams showing differentially expressed genes between *Otx2KO* ESCs (LIF+FBS) and WT ESCs (LIF+2i) both compared to WT EpiLCs (44hrs) (E, F), and between *Otx2KO* ESCs (LIF+FBS) and WT ESCs (LIF+FBS) both compared to WT ESCs (LIF+2i) (G, H). (I-L) RT-PCR assays of selected genes shown in Figure 4 are performed on two additional and independent RNA samples extracted from WT ESCs (LIF+2i), WT ESCs (LIF+FBS), WT EpiLCs (44hrs), *DKO* ESCs (LIF+FBS) and *Otx2KO* ESCs (LIF+FBS). (M-P) Comparative Venn diagrams performed to detect *DKO* transcripts in common with those specifically expressed in WT ESCs (LIF+2i) (red circles in box (**j**) in M, N), and *Otx2KO* transcripts in common with those selectively expressed in WT EpiLCs (44 hours) (red circles in box (**j**) in O, P). (Q, R) Venn diagram showing overlap between differentially expressed transcripts in *DKO* (LIF+FBS) *vs Otx2KO* (LIF+FBS) and the 500 NANOG responding genes (Festuccia et al., 2012) (Q), and Venn diagram between the 500 NANOG-sensitive genes (250 up- and 250 down-regulated) and the 608 OTX2-sensitive genes (230 up- and 378 down-regulated) both compared to control ESCs (R).

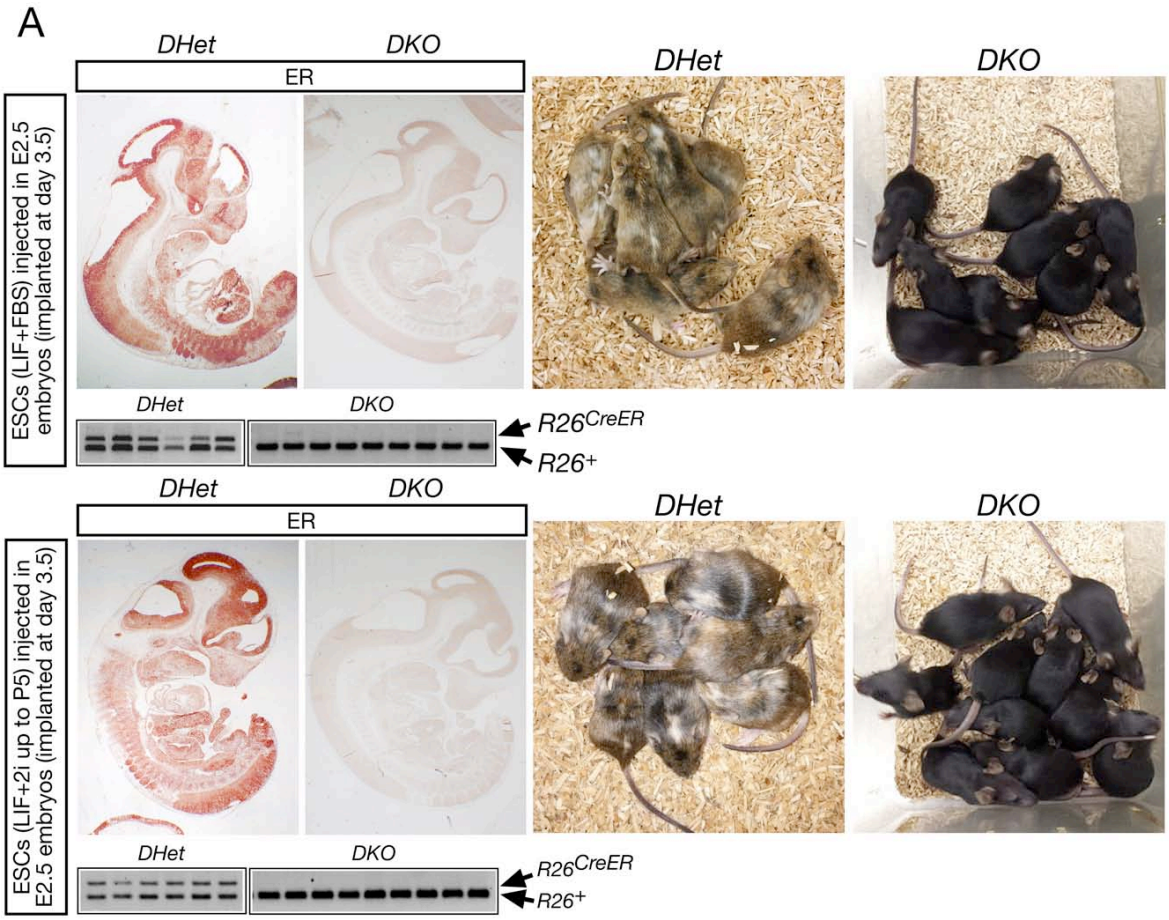

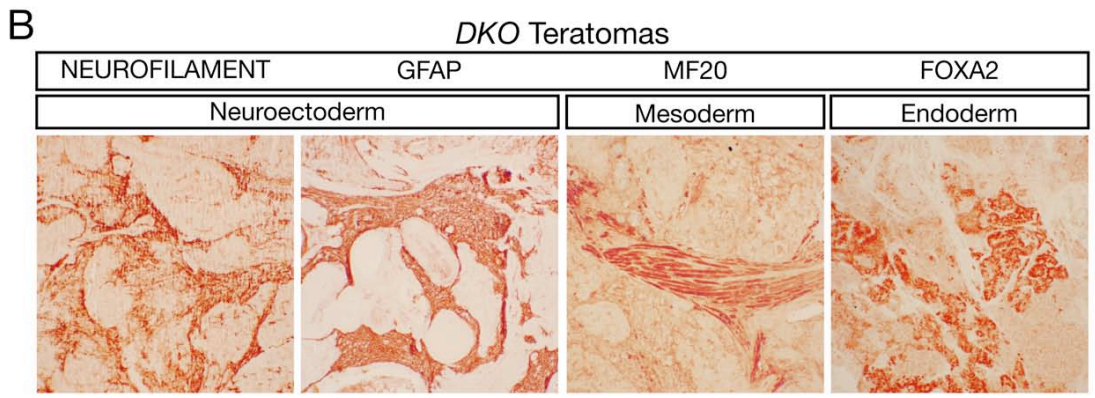

Figure S6. Chimerism ability and teratoma differentiation of *DKO* ESCs, related to Figure 5. (A) Host embryos are injected at E2.5 with *DHet* and *DKO* ESCs previously cultured in LIF+FBS or LIF+2i up to P5; chimerism is assessed at E12.5 by immunostaining with ER antibody and PCR assays on DNA from embryo tails, and in mice by coat color inspection; this analysis shows that, in contrast with *DHet* ESCs, the *DKO* ESC-derived progeny is not detected in embryos or postnatal mice. For each ESC line injected, the number of E12.5 embryos scored by immunohistochemistry is between 3 and 4, and the number of those scored by PCR is between 8 and 18; for postnatal chimerism, the number of scored mice is between 12 and 21 for each ESC line injected. (B) Representative immunohistochemistry assays performed on *DKO* ESC-derived teratoma with neurofilament, GFAP, MF20 and FOXA2 antibodies show that *DKO* ESCs generate neuroectodermal, mesodermal and endodermal derivatives (n=4 teratomas).

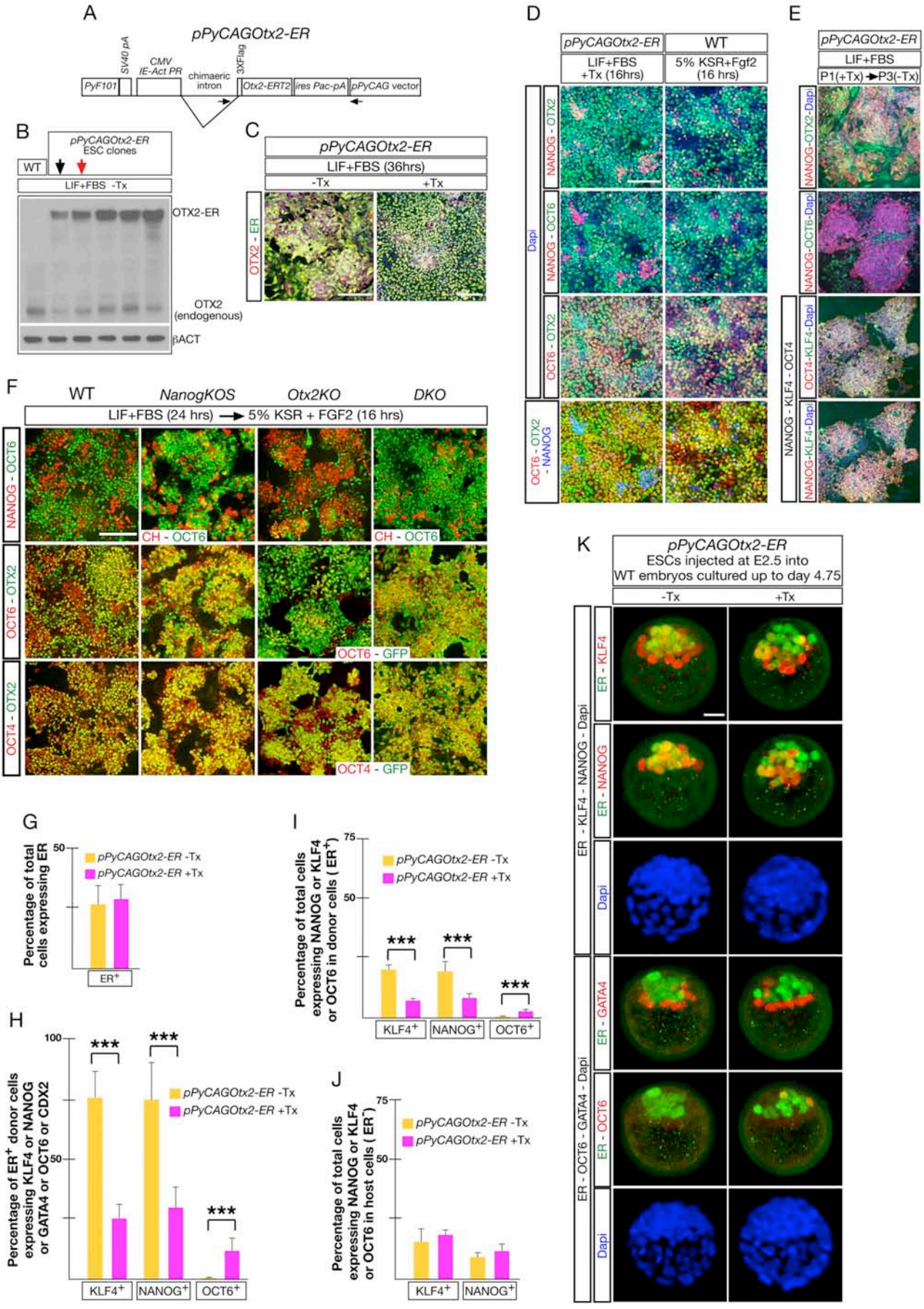

Figure S7. Generation and analysis of *pPyCAGOtx2-ER* ESCs and response to FGF2 of WT, *NanogKOS*, *Otx2KO* and *DKO* ESCs, related to Figure 6. (A) Schematic representation of the *pPyCAGOtx2-ER* construct transfected to generate mutant ESCs. (B) Western blot hybridized with the OTX2 antibody showing the expression level of the OTX2-ER transgene compared to that of the endogenous OTX2 in 5 independent mutant ESC lines including that selected for further analysis (red arrow); most of the experiments including cell counting are confirmed also in a second mutant ESC line (black arrow). (C) Representative immunostaining assays with OTX2 and ER of *pPyCAGOtx2-ER* ESCs treated or untreated with Tx show

nuclear internalization and ubiquitous expression of OTX2-ER in Tx-treated mutant ESCs. (D) Representative immunostaining assays with NANOG, OTX2 and OCT6 of *pPyCAGOtx2-ER* and WT ESCs plated as single cell suspension in presence of Tx or FGF2 and cultured for 16 hrs before fixation. (E) Representative immunostaining assays with NANOG and OTX2, NANOG and OCT6 and with NANOG, KLF4 and OCT4 show that Tx deprivation is sufficient to fully revert morphology of colonies and expression of markers to those exhibited by WT ESCs in LIF+FBS. (F) Representative images of WT, *NanogKOS*, *Otx2KO* and *DKO* ESCs cultured in LIF+FBS for 24 hrs, then treated with FGF2 for 16 hrs before immunostaining with NANOG or CH and OCT6, OTX2 or GFP and OCT6 and OTX2 or GFP and OCT4. (G) Graphic representation showing that embryos injected at E2.5 with *pPyCAGOtx2-ER* ESCs and cultured in presence or without Tx up to day 4.75 exhibit similar chimerism efficiency (n=10 for embryos cultured with or without Tx). (H) Cell counting showing the percentage of ER^+ ESCs co-expressing KLF4 or NANOG or OCT6 or GATA4 or CDX2. (I, J) Cell counting showing the percentage of total cells expressing NANOG or KLF4 or OCT6 in donor (ER^+) (I) or in host (ER^-) cells (J). For (I) and (J), n=7 blastocysts for each combination of antibodies and for each treatment (with or without Tx); (see also Table S6). (K) Representative confocal images showing immunostaining assays with ER, NANOG and KLF4 and with ER, OCT6 and GATA4 of chimeric blastocysts. Cells (C-E) or embryos (K) are also stained with Dapi. Data are presented as mean ± SD. Scale bar in C-F: 100µM; in K=30µM.

SUPPLEMENTAL TABLES

Table S1. Cell counting of WT, *NanogKO* and *NanogKOS* ESCs, related to Figures 1, S2 and S3

Cell number and percentage (mean ± s.d.) of ESC sub-types

Genotype	N° of Exps	Total cells	OCT4$^+$		KLF4$^+$ - OCT4$^+$		NANOG$^+$ (CH$^+$) - OCT4$^+$	
			N° of cells	% of total cells	N° of cells	% of OCT4$^+$ cells	N° of cells	% of OCT4$^+$ cells
WT	4	2594±140	2568±65	99±2	2314±143	89±5	2086±126	81±5
NanogKO	4	4582±483	620±144	13±3	77±18	12±3	223±40	36±6
NanogKOS	4	2263±61	1464±139	64±6	306±64	21±4	856±79	58±5
	N° of Exps	**Total cells**	**OCT4$^+$**		**OCT6$^+$ - OCT4$^+$**		**OTX2$^+$ - OCT4$^+$**	
			N° of cells	% of total cells	N° of cells	% of OCT4$^+$ cells	N° of cells	% of OCT4$^+$ cells
WT	4	2566±53	2524±55	98±2	469±47	18±2	1164±131	45±5
NanogKO	4	4675±571	691±171	15±4	437±56	63±8	483±48	70±7
NanogKOS	4	2153±56	1378±97	64±5	402±71	29±5	860±58	62±4

Triple IHC experiments with OTX2, NANOG or CH and OCT6 antibodies

	N° of Exps	Total cells (OCT4$^+$)	NANOG$^+$ (CH$^+$) - OTX2$^-$ - OCT6$^-$ (naïve-like)		NANOG$^+$ (CH$^+$) - OTX2$^+$ - OCT6$^-$ (pre-naïve-like)		NANOG$^-$ (CH$^-$) - OTX2$^+$ - OCT6$^-$ (unassigned)	
			N° of cells	% of total cells	N° of cells	% of total cells	N° of cells	% of total cells
WT	4	3039±149	1510±107	50±4	991±108	33±4	213±26	7±1
		Total cell sub-types (OCT4$^+$)	N° of cells	% of total cells	N° of cells	% of total cells	N° of cells	% of total cells
NanogKO	4	686±126	107±13	15±2	71±14	10±2	78±21	11±3
NanogKOS	4	1718±111	367±57	21±3	599±95	34±5	280±66	16±4
	N° of Exps	**Total cells (OCT4$^+$)**	**NANOG$^-$ (CH$^-$) - OTX2$^-$ - OCT6$^+$ (pre-primed-like)**		**NANOG$^-$ (CH$^-$) - OTX2$^+$ - OCT6$^+$ (primed-like)**		**NANOG$^+$ (CH$^+$) - OTX2$^+$ - OCT6$^+$ (new sub-type)**	
			N° of cells	% of total cells	N° of cells	% of total cells	N° of cells	% of total cells
WT	4	3039±149	298±49	10±2	214±22	7±1	8±3	0,2±0,1
		Total cell sub-types (OCT4$^+$)	N° of cells	% of total cells	N° of cells	% of total cells	N° of cells	% of total cells
NanogKO	4	686±126	98±19	14±3	283±48	41±7	84±19	12±3
NanogKOS	4	1718±111	222±59	13±3	214±48	12±3	70±27	4±2
	N° of Exps	**Total cells**	**Total cell sub-types (OCT4$^+$)**					
			N° of cells	% of total cells				
WT	4	3039±149	3233±268	106±8				
NanogKO	4	4379±474	686±126	16±3				
NanogKOS	4	2560±445	1718±111	67±4				

Table S2. Cell counting of WT, *DHet, Otx2KO, DKO, pPyCAGOtx2-ER and* WT (+FGF2) ESCs, related to Figures 3 and 6

Cell number and percentage (mean ± s.d.) of ESC sub-types

Genotype	N° of Exps	Total cells	OCT4$^+$		KLF4$^+$		NANOG$^+$ or CH$^+$	
			N° of cells	% of total cells	N° of cells	% of total cells	N° of cells	% of total cells
WT	4	2594±140	2568±65	99±2	2314±143	89±5	2111±118	81±5
DHet	4	2397±91	2361±103	98±5	2208±117	92±5	2033±126	85±5
Otx2KO	4	2536±69	2504±83	99±3	2434±101	96±4	2332±92	92±5
DKO	4	2228±106	2173±107	97±5	358±48	16±2	852±84	38±4
pPyCAGOtx2-ER	4	2716±111	2658±79	98±3	623±107	23±4	869±113	32±4
WT (+FGF2)	4	2207±103	2134±70	97±3	309±72	14±3	534±75	24±3
	N° of Exps	**Total cells**	**OCT4$^+$**		**OCT6$^+$**		**OTX2$^+$ or GFP$^+$**	
			N° of cells	% of total cells	N° of cells	% of total cells	N° of cells	% of total cells
WT	4	2566±53	2524±55	98±2	469±47	18±2	1164±131	45±5
DHet	4	2683±108	2636±111	98±4	296±49	11±2	995±115	37±4
Otx2KO	4	2193±58	2167±58	99±3	59±18	2,5±1	637±86	29±4
DKO	4	2503±104	2437±102	97±4	1601±131	64±5	2174±150	87±6
pPyCAGOtx2-ER	4	2531±80	2478±93	98±4	1793±159	71±6	2514±79	99±3
WT (+FGF2)	4	2326±138	2275±121	98±5	1302±121	56±5	1487±112	64±5

Triple IHC experiments with OTX2 or GFP, NANOG or CH and OCT6 antibodies

	N° of Exps	Total cells (OCT4$^+$)	NANOG$^+$ (CH$^+$) - OTX2$^-$ (GFP$^-$) - OCT6$^-$ (naïve-like)		NANOG$^+$ (CH$^+$) - OTX2$^+$ (GFP$^+$) - OCT6$^-$ (pre-naïve-like)		NANOG$^-$ (CH$^-$) - OTX2$^+$ (GFP$^+$) - OCT6$^-$ (unassigned)	
			N° of cells	% of total cells	N° of cells	% of total cells	N° of cells	% of total cells
WT	4	3039±149	1510±107	50±4	991±108	33±4	213±26	7±1
DHet	4	2553±195	1558±137	61±5	710±74	28±3	101±21	4±1
Otx2KO	4	2167±148	1519±136	70±6	461±66	21±3	201±21	9±1
DKO	4	2239±267	5±2 0,2±0,1		674±115	30±5	97±16	4±1
pPyCAGOtx2-ER	4	2289±90	N/A		434±73	19±3	251±31	11±1
WT (+FGF2)	4	2087±82	188±23	9±1	146±23	7±1	380±61	18±3
	N° of Exps	**Total cells (OCT4$^+$)**	**NANOG$^-$ (CH$^-$) - OTX2$^-$ (GFP$^-$) - OCT6$^+$ (pre-primed-like)**		**NANOG$^-$ (CH$^-$) - OTX2$^+$ (GFP$^+$) - OCT6$^+$ (primed-like)**		**NANOG$^+$ (CH$^+$) - OTX2$^+$ - OCT6$^+$ (new sub-type)**	
			N° of cells	% of total cells	N° of cells	% of total cells	N° of cells	% of total cells
WT	4	3039±149	298±49	10±2	214±22	7±1	8±3	0,2±0,1
DHet	4	2553±195	173±24	7±1	108±19	4±1	7±2	0,3±0,1
Otx2KO	4	2167±148	13±6 0,6±0,3		52±21	2,5±1	8±3	0,4±0,1
DKO	4	2239±267	275±43	12±2	1050±148	47±7	153±47	7±2
pPyCAGOtx2-ER	4	2289±90	N/A		1364±138	59±6	281±40	12±2
WT (+FGF2)	4	2087±82	338±49	16±2	776±78	37±4	274±46	13±2

Table S3. Up- and down- regulated gene transcripts detected in all comparisons, related to Figures 4 and S5. (Sheets 1-12) contain differentially expressed genes to identify the transcriptomic profile of *DKO* ESCs (LIF+FBS). (Sheets 13-24) contain differentially expressed genes to identify the transcriptomic profile of *Otx2KO* ESCs (LIF+FBS). (Sheet 25) contains up- and down-regulated genes identified in *DKO* ESCs (LIF+FBS) *vs Otx2KO* ESCs (LIF+FBS); the 264 NANOG responding genes reported in Figure S5Q are highlighted. (Sheet 26) contains the list of the 608 OTX2-sensitive genes (230 up- and 378 down-regulated) and the list of the 500 NANOG-sensitive genes (250 up- and 250 down-regulated) (Festuccia et al., 2012); genes that are down-regulated by loss of NANOG and up-regulated in the absence of OTX2 (n=18) are highlighted in pale blue, those with opposite expression profile (n=58) are highlighted in pink, and those down-regulated in both mutant ESC lines (n=6) are shown in green.
Note that differentially expressed genes reported in (Figures S5A-S5H) are highlighted in (Sheets 1-8, 11, 12, 17, 18, 21-24) (see excel file).

Table S4. List of up- and down regulated transcripts as they appear within each box of the Venn diagrams shown in Figures 4 and S5M-P, related to Figures 4 and S5. (Sheets 1-6) comparisons to identify the *DKO* ESCs (LIF+FBS) transcriptomic fraction in common with transcripts specifically up- or down-regulated in WT EpiLCs (44 hrs) (Sheets 1, 2), or in WT ESCs (LIF+FBS) (Sheets 3, 4), or in WT ESCs (LIF+2i) (Sheets 5, 6). (Sheets 7-12) comparisons to identify the *Otx2KO* ESCs (LIF+FBS) transcriptomic fraction in common with transcripts specifically up- or down-regulated in WT ESCs (LIF+FBS) (Sheets 7, 8), or in WT ESCs (LIF+2i) (Sheets 9, 10), or in WT EpiLCs (44 hours) (Sheets 11, 12) (see excel file).

Table S5. List of up and down-regulated gene transcripts reported in box (j) of each Venn diagram shown in Figures 4 and S5M-P, related to Figures 4 and S5. For each gene transcript is indicated the log2(FC). (see excel file).

Table S6. Cell counting in chimeric blastocysts, related to Figures 5 and S7

Genotype	N° of embryos	Total cells (Dapi$^+$)	ER$^+$ cells		N° of embryos	GATA4$^+$ cells	ER$^+$ cells	Total cells (Dapi$^+$)	GATA4$^+$ cells	GATA4$^+$ - ER$^+$ cells
		Mean ±sd	Mean ±sd	% ofTotal cells(±sd)		Mean ±sd	Mean ±sd	Mean ±sd	% of Total cells(±sd)	% of ER$^+$ cells(±sd)
DHet	10	73±5	20±5	28±8	7	11±2	19±4	71±4	15±3	0
Otx2KO	10	72±6	21±5	29±8	7	12±3	18±3	72±3	16±4	0
DKO	10	71±5	7±2	10±3	7	10±2	6±3	72±5	14±3	0
pPyCAGOtx2-ER (-TX)	10	74±6	17±4	23±6	7	12±2	16±4	71±6	20±4	0
pPyCAGOtx2-ER (+TX)	10	72±3	18±4	25±6	7	13±3	18±3	73±6	17±3	0

	N° of embryos	CDX2$^+$ cells	ER$^+$ cells	Total cells (Dapi$^+$)	CDX2$^+$ cells	CDX2$^+$ - ER$^+$ cells	OCT6$^+$ cells	ER$^+$ cells	Total cells (Dapi$^+$)	OCT6$^+$ cells	OCT6$^+$ - ER$^+$ cells
		Mean ±sd	Mean ±sd	Mean ±sd	% of Total cells(±sd)	% of ER$^+$ cells (±sd)	Mean ±sd	Mean ±sd	Mean ±sd	% of Total cells (±sd)	% of ER$^+$ cells(±sd)
DHet	7	44±6	19±2	73±4	59±8	0	0	20±3	74±5	0	0
Otx2KO	7	46±7	20±4	74±5	62±10	0	0	19±2	71±6	0	0
DKO	7	43±5	9±2	72±6	60±7	0	0	8±3	72±5	0	0
pPyCAGOtx2-ER (-TX)	7	47±6	15±3	74±5	62±8	0	0	16±4	71±6	0	0
pPyCAGOtx2-ER (+TX)	7	49±7	17±5	76±4	64±9	0	2±1	18±3	73±6	2±1	10±6

		KLF4$^+$ cells	ER$^+$ cells	Total cells (Dapi$^+$)	KLF4$^+$ cells	KLF4$^+$ - ER$^+$ cells		KLF4$^+$ - ER$^-$ cells
		Mean±sd	Mean±sd	Mean±sd	% of Total cells (±sd)	% of ER$^+$ cells (±sd)	% of Total cells (±sd)	% of Total cells (±sd)
	7	30±3	20±3	74±5	41±4	86±12	23±3	18±3
Otx2KO	7	29±4	19±3	71±6	42±6	87±12	25±3	17±4
DKO	7	18±5	8±3	72±5	25±6	22±14	2±1	23±7
pPyCAGOtx2-ER (-TX)	7	26±3	18±2	73±6	36±4	76±10	19±2	15±5
pPyCAGOtx2-ER (+TX)	7	18±2	17±5	74±6	24±3	25±6	6±1	18±2

		NANOG$^+$ cells	ER$^+$ cells	Total cells (Dapi$^+$)	NANOG$^+$ cells	NANOG$^+$ - ER$^+$ cells		NANOG$^+$ - ER$^-$ cells
		Mean±sd	Mean±sd	Mean±sd	% of Total cells (±sd)	% of ER$^+$ cells (±sd)	% of Total cells (±sd)	% of Total cells (±sd)
DHet	7	23±5	18±3	70±5	32±7	79±17	20±4	12±5
Otx2KO	7	24±4	18±4	73±3	33±5	89±21	22±5	11±2
DKO	7	10±2	8±3	72±5	14±3	0	0	15±3
pPyCAGOtx2-ER (-TX)	7	20±3	18±2	73±6	27±4	76±15	19±4	8±2
pPyCAGOtx2-ER (+TX)	7	14±2	17±5	74±6	18±3	30±8	7±2	11±3

		OTX2$^+$ cells	ER$^+$ cells	Total cells (Dapi$^+$)	OTX2$^+$ cells	OTX2$^+$ - ER$^+$ cells		OTX2$^+$ - ER$^-$ cells
		Mean±sd	Mean±sd	Mean±sd	% of Total cells (±sd)	% of ER$^+$ cells (±sd)	% of Total cells (±sd)	% of Total cells (±sd)
DHet	7	8±2	18±3	70±5	12±3	34±10	9±2	3±1
Otx2KO	7	3±2	18±4	73±3	4±3	0	0	4±2
DKO	7	4±1	8±3	72±5	5±1	0	0	5±1

		ER$^+$ cells	CH$^+$ (NANOG) - ER$^+$ cells		ER$^+$ cells	GFP$^+$ - ER$^+$ cells	
		Mean±sd	Mean±sd	% of ER$^+$ cells (±sd)	Mean±sd	Mean±sd	% of ER$^+$ cells (±sd)
DHet	7	23±5	18±4	78±17	23±5	9±3	39±14
Otx2KO	7	20±4	19±4	92±17	20±4	13±4	64±19
DKO	7	9±2	5±1	56±14	9±2	8±2	90±28

Table S7. List of primers and antibodies used in this study, related to Experimental Procedures. Primers are used for genotyping and expression analysis, antibodies for western blot and immunohistochemistry experiments. (see excel file).

SUPPLEMENTAL EXPERIMENTAL PROCEDURES

Generation of ESC lines

To obtain the *Otx2*$^{Gfp/-}$; *R26*$^{CreER/+}$ (*Otx2KO*) ESC line, a first *Otx2* allele was targeted with a *Gfp* cassette replacing the *Otx2* coding sequence; then a construct with no reporter gene was targeted in the *Otx2* WT allele, to obtain a second null allele lacking part of the *Otx2* 5'UTR and the genomic sequence spanning the entire coding region (Figure S1G). In the second ESC line, the *Gfp* reporter gene was targeted into a disrupted *Otx2* locus an then the *Ch* reporter gene was targeted into a disrupted *Nanog* locus, in order to generate the *Otx2*$^{Gfp/+}$; *Nanog*$^{Ch/+}$; *R26*$^{CreER/+}$ compound mutant (*DHet*) (Figure S1H). To generate a *Nanog* conditional allele, a targeting vector was designed, carrying three adjacent arms of homology, the intermediate of which contained the essential exons 2 and 3 flanked by two loxP sites. This molecule was introduced by homologous recombination in WT, *Otx2*$^{Gfp/+}$, and *Otx2KO* ESCs, thus generating the *Nanog*$^{flox/+}$; *R26*$^{CreER/+}$ and *Nanog*$^{flox/+}$; *Otx2*$^{Gfp/-}$; *R26*$^{CreER/+}$ cell lines, respectively. The *Nanog* WT locus of these three cell lines underwent an additional round of *Ch* targeting, which gave rise to the *Nanog*$^{flox/Ch}$; *R26*$^{CreER/+}$ (*NanogCKO*) (Figure S1B), and *Nanog*$^{flox/Ch}$; *Otx2*$^{Gfp/-}$; *R26*$^{CreER/+}$ *(NanogCKO; Otx2KO*) ESC lines (Figure S1D). Inactivation of the *Nanog*^{flox} allele and removal of the *neo* cassette was obtained, as last step, by Tx administration (200nM) to the three conditional ESC lines in order to generate *NanogKO* (Figure S1C) and *DKO* (Figure S1E) mutant ESCs. In all cases, correct targeting and *loxP* sites recombination events were respectively monitored by Southern blots (data not shown) and allele specific PCRs (Figures S1I) using the primers indicated in each mutant line. Primers are shown in Table S7. Mutant *pPyCAGOtx2-ER* ESC lines were obtained by transfecting WT ESCs with a linearised plasmid expressing an OTX2-ER fusion protein under the transcriptional control of the combined hCMV immediate early enhancer and chicken *β-Actin* promoter (Figure S7A). Randomly isolated clones were screened for transgene expression by Western blot and two clones (black and red arrows in Figure S7B) were selected for subsequent analysis. OTX2-ER nuclear translocation was induced by Tx administration (200 nM).

Cell culture experiments

Routine ESC culture was performed in Glasgow Minimal Essential Medium (GMEM, SIGMA) plus 12% FBS (Hyclone) and LIF (300U/ml Millipore). Inactivation of the *Nanog*^{flox} allele and deletion of the *neo* cassette downstream of the *Ch* gene (*NanogCKO* and *NanogCKO; Otx2KO*) was obtained by administration of Tx (200 nM) 3 hours upon cell plating at a cloning density. Tx was removed on the day of picking and single clones were analysed for loxP recombination by PCR. For *NanogKO* and *DKO*. More than 95% of clones fully inactivated *Nanog* but very few of them can be passaged over 12 times. As for the experiments involving small-molecule inhibitors, ESCs grown in LIF+FBS were plated in N2B27 medium with LIF (300 U/ml), supplemented with 1mM MEK1/2 inhibitor PD325901 (PD, Calbiochem) and with 3mM GSK3 inhibitor CHIR99021 (CHIR, Calbiochem) (Buecker et al., 2014). These cells were referred to as passage 1 (P1) and were propagated approximately every three days by accutase treatment. EpiLCs were induced from ESCs as previously described (Brons et al., 2007; Acampora et al., 2013) and analyzed at 44 hours for RNA-seq experiments. For early priming experiments, ESCs maintained in LIF, were cultured in GMEM supplemented with 5% knockout serum replacement (KSR, Invitrogen) and FGF2 (12 ng/ml) for additional 16 hours (Acampora et al., 2013).

RNA-seq experiments, analysis of RNA-seq data and RNA-seq validation assays

Indexed sequencing libraries were generated from 1mg of total RNA by using the TruSeq Stranded Total RNA Sample Prep Kit with Ribo-Zero ribosomal RNA reduction chemistry (Illumina, San Diego, CA) (Acampora et al., 2016). Electrophoresis of the libraries on Bioanalyzer 2100 instrument (Agilent, Santa Clara, CA) showed highest peaks at 230–270 bp. A total of 65-84 Million PE reads for each sample were generated. Raw FASTQ reads were analyzed as described (Acampora et al, 2016) from the Illumina BaseSpace environment (basespace.illumina.com) using TopHat 2 aligner to align reads and Cufflinks 2.1.1 to analyse gene-level raw count values. Differentially expressed genes were further filtered by q-value < 0.05 and by change magnitude ($|\text{fold change}| \geq 1.5$). RNA-seq data were validated by semi-quantitative RTPCR assays. Amongst those with high score in expression fold change (both up- and down-regulated), a representative number of genes was randomly chosen from the gene list reported in box (**j**) highlighted by red circle in Figures 4A-4D and Tables S3-S5. Primers and cycles were listed in Table S7.

Chimerism experiments

Mid-gestation and adult chimeras were obtained by injecting 10-15 ESCs, grown in LIF+FBS or LIF+2i media up to P5, into C57BL/6 E2.5 (8 cell stage) embryos allowed to develop *in vitro* for additional 24-30 hrs before implantation. Chimerism was evaluated at E12.5 by PCR monitoring the ratio between *R26* WT and *R26*^{CreER} allele amplification and by CreER immunostaining. Chimerism was also assessed post-natally by coat color inspection.

For experiments involving cell counting on preimplantation chimeric embryos, ESCs grown in LIF+FBS were injected into E2.5 embryos, cultured for about 50 hours (up to day 4.75) in KSOM (Millipore) and analysed by immunostaining as previously described (Acampora et al., 2016). For *pPyCAGOtx2-ER* the E2.5 injected embryos were cultured up to day 4.75 with or without Tx (200nM).

Teratomas were generated by subcutaneous injection of 1.5×10^6 *DKO* ESCs into athimic nude mice.

Cell counting experiments

For cell counting performed on *in vitro* experiments, control and mutant ESCs were dissociated and plated at high density as single cell suspension in chamber slides. Cells were allowed to adhere for 8-10 hours before to be fixed and immunostained. FGF2-treated WT and Tx-treated pPyCAGOtx2-ER ESCs were plated as single cell suspension at high density in presence of

FGF2 or Tx and cultured for 16 hrs before fixation. Immunohistochemistry images on cultured ESCs were acquired by using a Nikon eclipse NI microscope. For immunohistochemistry experiments performed with 3 compatible antibodies, fluorescence was excited at 405 nm for Dapi and at 488 nm, 555 nm and 647 nm for secondary antibodies. Eventually, red color for fluorence excited at 555 nm was converted to green or blue pseudocolors to allow merging of all combinations.
For cell counting experiments on blastocysts, laser scanning confocal images of immunostained blastocysts were acquired on a Nikon A1R by using a Plan-apochromat 20X/NA 0.75 objective. Optical section tickness ranged from 2 to 4 µm and 12-15 planes were acquired for each blastocyst. Confocal 3D reconstructed images were used for manual cell counting of $Dapi^+$ total cells or ER^+ or ER^- cells co-expressing or not NANOG, OTX2, CH, GFP, KLF4, OCT6, GATA4 and CDX2.

SUPPLEMENTAL REFERENCES

Acampora, D., Di Giovannantonio, L.G., and Simeone, A. (2013). Otx2 is an intrinsic determinant of the embryonic stem cell state and is required for transition to a stable epiblast stem cell condition. Development *140*, 43-55.

Acampora, D., Omodei, D., Petrosino, G., Garofalo, A., Savarese, M., Nigro, V., Di Giovannantonio, L. G. and Simeone, A. (2016) Loss of the Otx2-binding site in the Nanog promoter affects the integrity of embryonic stem cell subtypes and specification of inner cell mass-derived epiblast. Cell Rep. *15*, 2651-2664.

Brons, I.G., Smithers, L.E., Trotter, M.W., Rugg-Gunn, P., Sun, B., Chuva de Sousa Lopes, S.M., Howlett, S.K., Clarkson, A., Ahrlund-Richter, L., Pedersen, R.A. et al. (2007). Derivation of pluripotent epiblast stem cells from mammalian embryos. Nature *448*, 191-195.

Buecker, C., Srinivasan, R., Wu, Z., Calo, E., Acampora, D., Faial, T., Simeone, A., Tan, M., Swigut, T., and Wysocka, J. (2014). Reorganization of enhancer patterns in transition from naive to primed pluripotency. Cell Stem Cell *14*, 838-853.